



This is a repository copy of *Dramatic impact of the TiO<sub>2</sub> polymorph on the electrical properties of 'stoichiometric' Na<sub>0.5</sub>Bi<sub>0.5</sub>TiO<sub>3</sub> ceramics prepared by solid-state reaction.*

White Rose Research Online URL for this paper:

<https://eprints.whiterose.ac.uk/182414/>

Version: Supplemental Material

---

**Article:**

Yang, F., Hu, Y., Hu, Q. et al. (6 more authors) (2022) Dramatic impact of the TiO<sub>2</sub> polymorph on the electrical properties of 'stoichiometric' Na<sub>0.5</sub>Bi<sub>0.5</sub>TiO<sub>3</sub> ceramics prepared by solid-state reaction. *Journal of Materials Chemistry A*, 10 (2). pp. 891-901. ISSN 2050-7488

<https://doi.org/10.1039/d1ta09668k>

---

© 2021 The Royal Society of Chemistry. This is an author-produced version of a paper subsequently published in *Journal of Materials Chemistry A*. Uploaded in accordance with the publisher's self-archiving policy.

**Reuse**

Items deposited in White Rose Research Online are protected by copyright, with all rights reserved unless indicated otherwise. They may be downloaded and/or printed for private study, or other acts as permitted by national copyright laws. The publisher or other rights holders may allow further reproduction and re-use of the full text version. This is indicated by the licence information on the White Rose Research Online record for the item.

**Takedown**

If you consider content in White Rose Research Online to be in breach of UK law, please notify us by emailing [eprints@whiterose.ac.uk](mailto:eprints@whiterose.ac.uk) including the URL of the record and the reason for the withdrawal request.



[eprints@whiterose.ac.uk](mailto:eprints@whiterose.ac.uk)  
<https://eprints.whiterose.ac.uk/>

## Supplementary Information

### **Dramatic impact of the TiO<sub>2</sub> polymorph on the electrical properties of ‘stoichiometric’ Na<sub>0.5</sub>Bi<sub>0.5</sub>TiO<sub>3</sub> ceramics prepared by solid-state reaction**

Fan Yang<sup>1,#,\*</sup>, Yidong Hu<sup>2,#</sup>, Qiaodan Hu<sup>2,\*</sup>, Sebastian Steiner<sup>3</sup>, Till Frömling<sup>3</sup>, Linhao Li<sup>4</sup>, Patrick Wu<sup>4</sup>, Emilio Pradal-Velázquez<sup>4</sup> and Derek C Sinclair<sup>4,\*</sup>

<sup>1</sup> Institute of Fuel Cells, School of Mechanical Engineering, Shanghai Jiao Tong University, 800 Dongchuan Road, Minhang District, Shanghai, 200240, P. R. China.

<sup>2</sup> School of Materials Science and Engineering, Shanghai Jiao Tong University, 800 Dongchuan Road, Minhang District, Shanghai, 200240, P. R. China

<sup>3</sup> Department of Materials and Earth Science, Technical University of Darmstadt, FB Nichtmetallisch-Anorganische Werkstoffe, Alarich-Weiss-Straße 2, D-64287 Darmstadt, Germany

<sup>4</sup> Department of Materials Science and Engineering, University of Sheffield, Sir Robert Hadfield Building, Mappin Street, Sheffield, S1 3JD, UK.

\*Corresponding authors.

[fanyang\\_0123@sjtu.edu.cn](mailto:fanyang_0123@sjtu.edu.cn); [qdhu@sjtu.edu.cn](mailto:qdhu@sjtu.edu.cn); [d.c.sinclair@sheffield.ac.uk](mailto:d.c.sinclair@sheffield.ac.uk)

# Equally contributed authors.

#### **1. Comparison of the electrical conductivity of NBT ceramics sintered with and without binder**

Here two methods were used to sinter dense NBT ceramics, including 1) uni-axial cold pressing followed by isostatic pressing at 200 MPa (denoted as “cip”) and 2) uni-axial pressing with a 5 wt.% water solution of polyvinyl alcohol (PVA) as binder without isostatic pressing (denoted as “binder”). Fig.S1 compares the bulk conductivity ( $\sigma_b$ ) of Bi-deficient NBT (NB<sub>0.49</sub>T), nominally stoichiometric NBT (NB<sub>0.50</sub>T) and Bi-excess NBT (NB<sub>0.51</sub>T) prepared by the above two methods. These ceramics were all prepared using rutile TiO<sub>2</sub>. Fig.S1 shows use of binder causes a slight decrease of  $\sigma_b$  of NB<sub>0.50</sub>T without changing the  $\sigma_b$  -1000/T relationship. The two sintering methods do not cause the significantly different electrical conductivity of NB<sub>0.50</sub>T prepared using rutile and anatase TiO<sub>2</sub>, and therefore do not influence the major conclusion of this work.

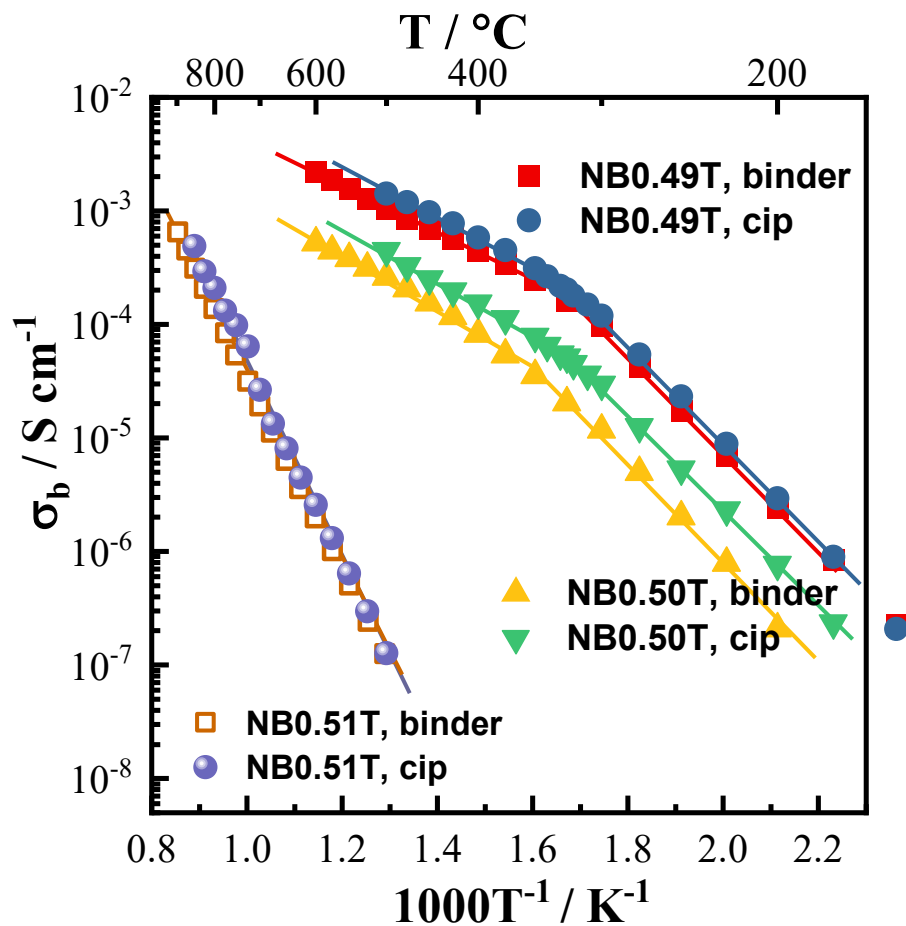


Figure S1. Arrhenius plots for  $\sigma_b$  of Bi-deficient NBT (NB<sub>0.49</sub>T), nominally stoichiometric NBT (NB<sub>0.50</sub>T) and Bi-excess NBT (NB<sub>0.51</sub>T). All ceramics were prepared by rutile TiO<sub>2</sub>. “cip” represents uni-axial cold pressing followed by isostatic pressing. “binder” represents uni-axial cold pressing with PVA as a binder without isostatic pressing.

## 2. XRD patterns of NBT ceramics prepared from different reagents

Fig.S2 shows the XRD patterns of NBT ceramics prepared by different reagents. The numbers after NBT represent different combinations of  $\text{Na}_2\text{CO}_3$ ,  $\text{Bi}_2\text{O}_3$  and  $\text{TiO}_2$  reagents from Table 1 in the main text. All NBT ceramics are phase pure with a rhombohedral structure.

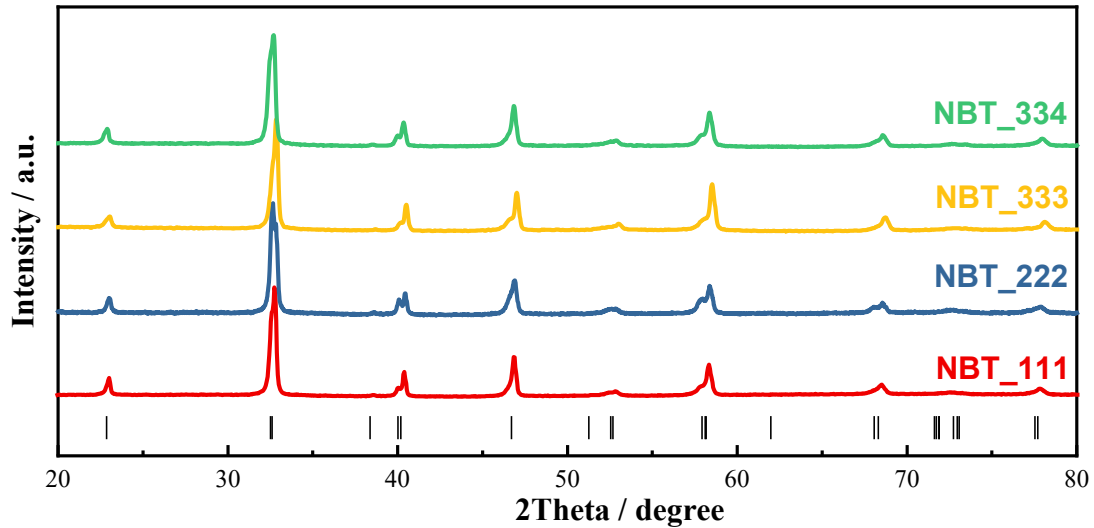


Figure S2. XRD patterns of sintered NBT ceramics prepared by different reagents. The vertical lines below the patterns represent the peak positions for NBT with a rhombohedral structure.

### 3. Full synchrotron XRD patterns in the $2\theta$ range between $15-85^\circ$

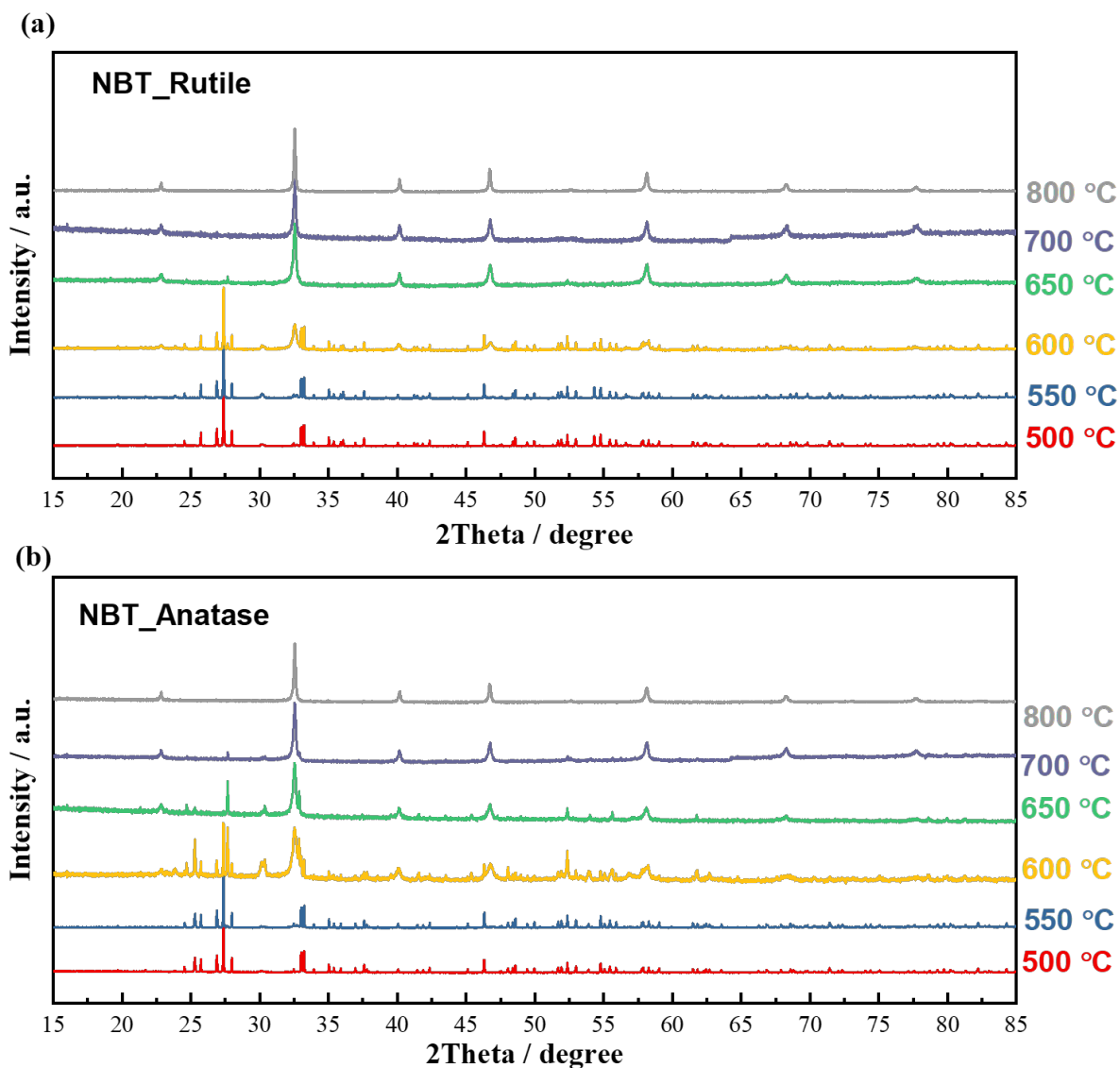


Figure S3. Evolution of the XRD patterns with calcination temperature in the  $2\theta$  range between  $15-85^\circ$ . (a) Mixture with rutile  $\text{TiO}_2$  and (b) with anatase  $\text{TiO}_2$ .

#### 4. Particle size distribution

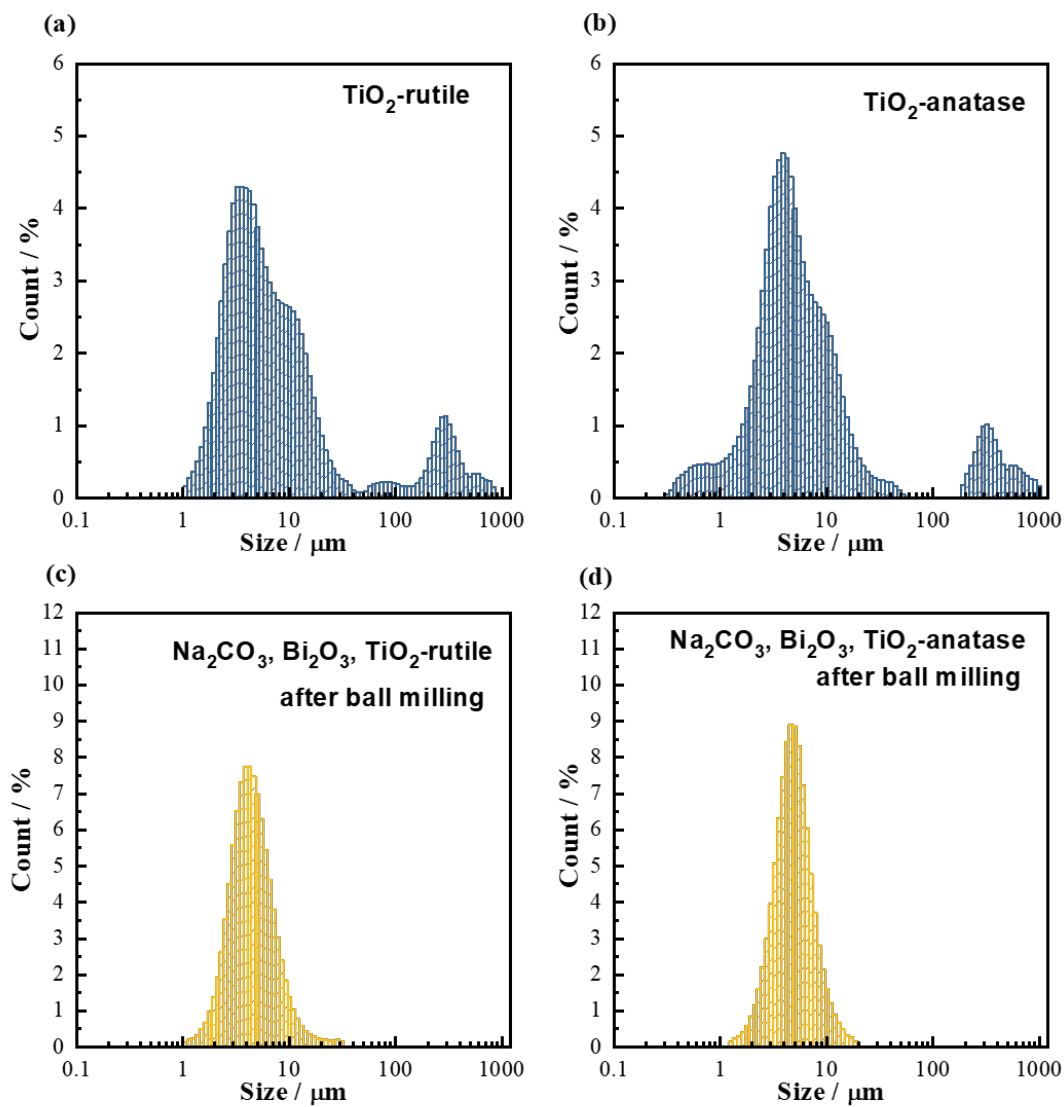


Figure S4. Particle size distribution of (a) raw rutile TiO<sub>2</sub>, (b) raw anatase TiO<sub>2</sub>, (c) ball-milled and sieved mixture of pre-dried Na<sub>2</sub>CO<sub>3</sub>, Bi<sub>2</sub>O<sub>3</sub> and rutile TiO<sub>2</sub>, and (d) ball-milled and sieved mixture of Na<sub>2</sub>CO<sub>3</sub>, Bi<sub>2</sub>O<sub>3</sub> and anatase TiO<sub>2</sub>.

## 5. Evolution of $\text{Bi}_2\text{O}_3$ , $\text{Bi}_{12}\text{TiO}_{20}$ and NBT fractions during solid-state reaction

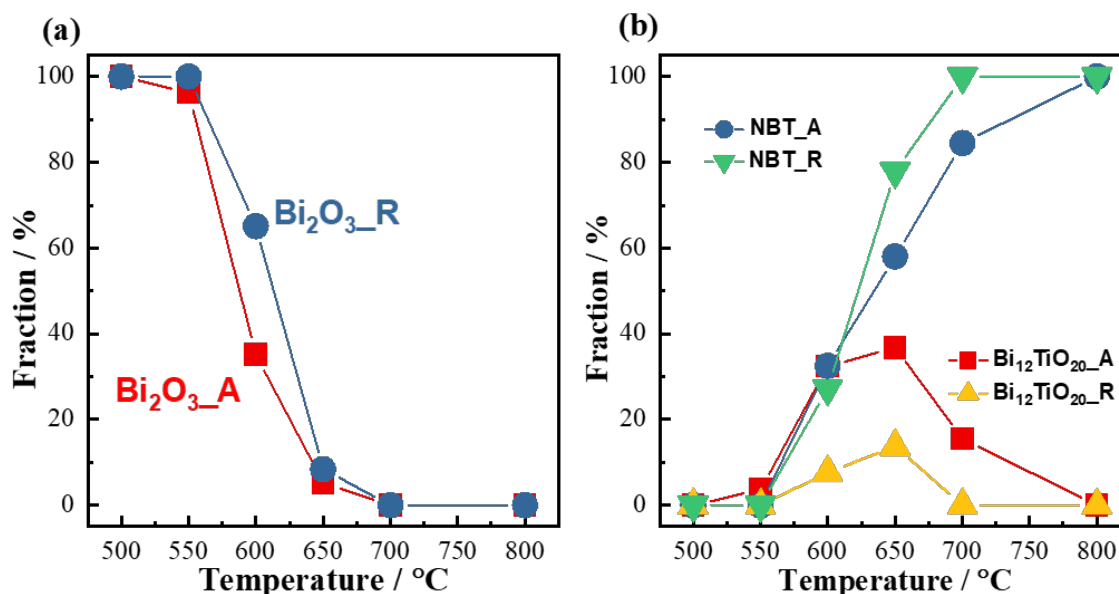


Figure S5. Evolution of the fraction parameter of Bi-containing phases during solid-state reaction when rutile and anatase  $\text{TiO}_2$  are used as reagents. (a)  $\text{Bi}_2\text{O}_3$ , (b)  $\text{Bi}_{12}\text{TiO}_{12}$  and NBT.

## 6. Impedance spectroscopy of $\text{NBT}_{\text{R}0.5\text{A}0.5}$

Impedance data for  $\text{NBT}_{\text{R}0.5\text{A}0.5}$  are presented in Nyquist (Fig.S6a) and Bode ( $M''$ - $\log f$ , Fig.S6b) plots.  $Z^*$  plots for  $\text{NBT}_{\text{R}0.5\text{A}0.5}$  at 500 °C show two poorly resolved arcs and a low-frequency spike corresponding to an electrode effect. The electrode spike is characteristic of ionic conduction behavior. With increasing temperature, the two arcs gradually merge into one suggesting a different activation energy for the two responses.  $M''$ - $\log f$  plots at lower temperatures, e.g., 300 °C, show a broad peak, suggesting an inhomogeneous electrical microstructure for  $\text{NBT}_{\text{R}0.5\text{A}0.5}$ . The  $M''$ - $\log f$  peak height increases with increasing temperature suggesting a reduced relative permittivity with increasing temperature between 300 – 700 °C. The inhomogeneous electrical microstructure agrees with the random distribution of large and small grains, as shown in Fig.6c.

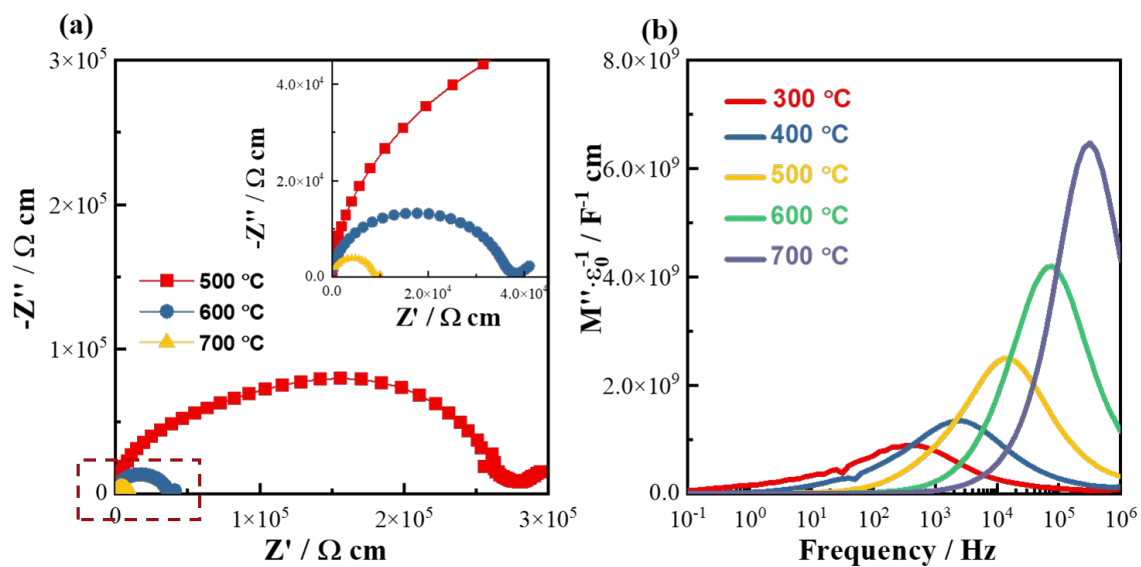


Figure S6. Impedance data for NBT<sub>R0.5A0.5</sub>. (a)  $Z^*$  plots at 500, 600 and 700 ° C and (b)  $M''$ -log $f$  plots at 300-700 ° C at increments of 100 ° C. The inset figure in (a) is an expanded view of the rectangular region.